Polymer Chemistry

ROYAL SOCIETY OF CHEMISTRY

REVIEW

View Article Online
View Journal | View Issue

Cite this: *Polym. Chem.*, 2020, **11**, 3673

Polymerization techniques in polymerization-induced self-assembly (PISA)

Chao Liu, Chun-Yan Hong * and Cai-Yuan Pan*

The development of controlled/"living" polymerization greatly stimulated the prosperity of the fabrication and application of block copolymer nano-objects. Controlled/"living" polymerization was later extended to the scope of polymerization-induced self-assembly (PISA), in which a linear increase of the solvophobic blocks resulted in systemic variation of the packing parameter and almost ergodic morphology transitions. PISA combines polymerization and self-assembly in a much concentrated solution, which has been demonstrated to be a powerful strategy for fabricating block copolymer nano-objects. Various controlled/"living" polymerization techniques, such as reversible addition–fragmentation chain transfer (RAFT) polymerization, nitroxide-mediated polymerization (NMP), atom transfer radical polymerization (ATRP), "living" anionic polymerization, and ring-opening metathesis polymerization (ROMP), have been used in PISA to date. In this review, we summarize the developments of polymerization techniques in PISA, which complementarily enlarge the scope of PISA to a broad range of reaction conditions and monomer families.

Received 28th March 2020,
Accepted 6th May 2020

DOI: 10.1039/d0py00455c

rsc.li/polymers

1. Introduction

The self-assembly of block copolymers (BCPs) is a well-known strategy to prepare a wide range of nano-objects, including spheres, worms, lamellae and vesicles,[1–6] which have shown promising potential and practical applications in biomedicine, nanoreactors, catalysis, and so on.[7–11] The development of controlled/"living" polymerization offers opportunities to fabricate various well-defined amphiphilic block copolymers, which greatly stimulated the research of self-assembly of BCPs to fabricate polymeric nano-objects. Traditional BCP self-assembly is typically conducted in a dilute solution *via* a post-polymerization process, which involves redundant multiple steps.[12–15] This tedious and low-efficiency process is a significant limitation for the scale-up preparation of BCP nano-objects and hence hampers their potential commercial applications. Polymerization-induced self-assembly (PISA) offers an attractive solution to the above-mentioned limitations. In principle, PISA can be performed *via* dispersion polymerization or aqueous emulsion polymerization. Aqueous emulsion

CAS Key Laboratory of Soft Matter Chemistry, Department of Polymer Science and Engineering, University of Science and Technology of China, Hefei, Anhui 230026, P. R. China. E-mail: hongcy@ustc.edu.cn, pcy@ustc.edu.cn

Chao Liu

Chao Liu is currently a postdoctoral fellow at the University of Science and Technology of China (USTC). He received his Ph.D. in chemistry from USTC in 2019 under the supervision of professors Chun-Yan Hong and Cai-Yuan Pan. He then joined Prof. Yezi You's group as a postdoctoral fellow in July 2019. His scientific interest is focused on the synthesis of topological polymers and polymerization-induced self-assembly.

Chun-Yan Hong

Chun-Yan Hong is a professor at the University of Science and Technology of China (USTC). She obtained her Ph.D. in chemistry from USTC in 2002. Her research interests include controlled radical polymerization, the synthesis of stimuli responsive polymers and biodegradable polymers, the fabrication of functionalized nanomaterials, and their applications in drug or gene delivery.

polymerization is realized by chain extension with a water-immiscible monomer from a water-soluble polymer chain, with advantages of high polymerization rate as well as high monomer conversion.[16–23] Due to the use of water as the reaction medium and the versatility to obtain a large library of monomers, emulsion polymerization has attracted extensive attention. The big difference between the spheres formed in emulsion polymerization and in dispersion polymerization is the random arrangement of polymer chains in the former case and ordered arrangement of polymer chains in the latter case although they are composed of the same BCP because the emulsion spheres are formed by extending polymerization of the hydrophilic polymeric stabilizer on the monomer droplets, which does not undergo macromolecular self-assembly but such a self-assembly occurs in dispersion polymerization. With chain growth of the second block, the ordered BCP chains in the spherical micelles are relatively easy to reorganize forming various morphologies in dispersion polymerization, however, the BCP chains in the spheres formed through various nucleation mechanisms are difficult to reorganize forming higher-order morphologies due to the entangling of polymer chains in the emulsion polymerization. To date, it is not clear how to control the self-assembly as a sole nucleation through changing the conditions of emulsion polymerization. Recent progress has been made in addressing this problem by designing hydrophilic stabilizer blocks, regulating monomer solubility, reaction parameters and radical initiator concentration for facilitating the formation of nonspherical higher-order morphologies in emulsion polymerization.[24–28] Therefore, the adopted polymerization techniques in the PISA process are often conducted under dispersion polymerization. In this review, we discuss recent progress in various polymerization techniques in PISA with an emphasis on dispersion polymerization, and emulsion polymerizations with morphology transitions or self-assembly nucleation are included.

For a typical PISA process in dispersion polymerization, a soluble precursor acting as a macro-initiator and stabilizer simultaneously is chain-extended *via* the polymerization process of the soluble second monomer.[29–35] As the chain-extension proceeds, the growing second block eventually becomes insoluble at some critical degree of polymerization (DP), generally forming spherical micelles first. Continuous polymerization of the second block drives the reorganization of the BCP chains to form nano-objects with different morphologies.[36–40] However, the kinetically entrapped spheres are usually obtained in original PISA examples, and the polymerization-induced reorganization of spheres to form other higher ordered morphologies is greatly limited due to the low chain mobility of the solvophobic blocks.[41–43] The first example to achieve morphological transition of spheres to a higher order morphology in RAFT dispersion PISA is reported by our group.[44] Excess styrene was used as the monomer and the co-solvent, and the residual styrene plasticized the spherical micelles which lowered the T_g of the solvophobic blocks in the solvent (hereinafter, defined as T_{sg}) to below the polymerization temperature. Almost simultaneously, PISA-generated polymeric nano-objects with higher morphologies (worms or vesicles) in emulsion polymerization were reported by Charleux and coworkers.[45] Subsequently, Armes and coworkers reported that vesicles with low T_{sg} were generated in PISA.[46] In comparison with the T_g of the polymer in the dry state, the solvated T_g (T_{sg}) is a much more important parameter in PISA, which has been attracted increasing attention recently. Basically, the polymerization should be carried out at a higher temperature than T_{sg} to obtain sufficient chain mobility of the solvophobic block for morphological transition. Morphological transitions from spheres to various higher order morphologies, such as worms/rods, lamellae, toroids, vesicles, and other more complex morphologies, have been achieved in PISA.[47–51] In comparison with the conventional self-assembly strategy, PISA can be performed at a relatively high solid content (up to 50% w/w), and the preparation can be easily realized in a one-pot manner rather than using a tedious post-modification process, which offers a highly versatile approach to construct block copolymer nano-objects.

Varying the composition of the solvents to adjust the solubility of one block is usually used to drive the self-assembly of amphiphilic BCPs in the traditional self-assembly strategy. However, the composition of solvents is almost unchanged in most cases of PISA, and the major driving force to induce self-assembly in PISA is the growing chain length of the solvophobic blocks. The growth of the well-defined block copolymers with low molecular weight distribution causes systemic variation of the packing parameter and ergodic morphology transitions. Controlled/"living" polymerization to generate well-defined block copolymers is one of the basic principles of PISA, although a few examples of deliberately increasing the molecular weight distribution for fine-tuning of the nano-objects have been reported.[52–55] For example, Armes *et al.* used a binary mixture of a relatively long and a relatively short poly (methacrylic acid) stabilizer block in RAFT dispersion polymerization of benzyl methacrylate (BzMA), and vesicles with low-polydispersity were obtained.[52] All controlled/"living" polymerization mechanisms can be applied to PISA in principle, such as reversible addition–fragmentation chain transfer (RAFT)

Cai-Yuan Pan

Cai-Yuan Pan joined the University of Science and Technology of China as a lecturer in 1977 and became a full professor in 1989. His interests include the synthesis and characterization of polymers, especially those with different topological structures, and the preparation and properties of nanomaterials.

Table 1 Main polymerization techniques in PISA

Polymerization techniques[a]	Monomers	Morphologies	Ref.
RAFT	Methacrylate, acrylate, methacrylamide, acrylamide, styrene	Spheres, worms, lamellae, vesicles, jellyfish	56–63
NMP	Methacrylate, acrylate, acrylamide, styrene	Spheres, worms, vesicles	64–76
ATRP	Methacrylate, acrylate acrylamide, styrene	Spheres, worms, vesicles	77–91
LAP	Isoprene, styrene, styrenic	Spheres, worms, vesicles	92–98
ROMP	Norbornene, cyclooctatetraene, 1,5-cyclooctadiene	Spheres, worms, vesicles	99–117
ROP	*N*-Carboxyanhydride	Worms, vesicles	178 and 179
TERP	Methacrylate, acrylate, styrene	Spheres	184–189
IMP	Methacrylate	Spheres, worms, vesicles	190–192

[a] Abbreviations: RAFT, reversible addition–fragmentation chain transfer; NMP, nitroxide mediated polymerization; ATRP, atom transfer radical polymerization; LAP, living anionic polymerization; ROMP, ring-opening metathesis polymerization; ROP, ring-opening polymerization; TERP, organotellurium-mediated radical polymerization; IMP, iodine-mediated polymerization.

polymerization,[56–63] nitroxide-mediated polymerization (NMP),[30,64–76] atom transfer radical polymerization (ATRP),[77–91] living anionic polymerization,[92–98] or ring-opening metathesis polymerization (ROMP)[99–117] (Table 1), because all these polymerizations displayed linear increase of the second block length with the conversion increase. Due to the progressive increase of the second block, the controlled/"living" polymerizations in a selective solvent form always spherical micelles at first, and then continuous growth of the second block length drives reorganization of BCP chains, forming nano-objects with various morphologies.[47,48,118,119] Obviously, nano-objects besides spherical micelles are formed *via* two processes, polymerization-induced self-assembly and polymerization-induced reorganization, not just only *via* the PISA process based on the definition of self-assembly.[120,121] In this review, we summarize and discuss the developments on the fabrication of various nano-objects (excluding only the formation of spherical micelles) *via* the PISA process mediated by controlled/"living" polymerization mechanisms. Thus, the term "PISA" used in this review includes two process, polymerization-induced self-assembly and reorganization.

2. RAFT polymerization

Among controlled/"living" polymerizations, RAFT polymerization is the predominantly used technique in PISA to date due to its tolerance to a broad range of reaction conditions and monomer families. In addition, according to the polymerization media, the polymerization can be carried out in water and in organic solvents, and these two types of solvents have been extensively used in RAFT dispersion polymerization for the preparation of the nano-objects.[122–127]

2.1. Thermally initiated RAFT Polymerization

2.1.1. Organic solvents. Most of the RAFT dispersion polymerizations used for the preparation of various nano-objects were conducted in organic solvents, including lower alcohols, and alkanes,[122,126,128,129] even some less commonly used solvents such as supercritical CO_2, ionic liquids, and poly(ethylene glycol)s.[130–132] Among these solvents, alcohols are the most used solvent. In 2009, our group was the first to report the preparation of nonspherical morphologies by PISA using RAFT-mediated dispersion polymerization.[44] The polymerization of styrene was performed in methanol in the presence of different macro chain transfer agents (macro-CTAs) including poly(4-vinylpyridien) (P4VP), poly(ethylene oxide) (PEO), poly [2-(*N*,*N*-dimethylamino)ethyl methacrylate] (PDMAEMA), and poly(acryl acid) (PAA).[118,119,133–135] Various morphologies, such as nanorods, fibers, vesicles, large-compound vesicles, spaced concentric vesicles, and hexagonally packed hollow hoops, have been fabricated.[47,48,129] The TEM and DLS results revealed that spherical micelles were formed initially, and then polymer chains in the aggregates were reorganized to form nanorods or vesicles. In those early reports, in order to achieve morphological transition, a high feed ratio of St to macro-CTA was usually employed to plasticize the core-forming blocks and retain the propagation, thus the monomer conversions were generally low. In order to enhance the monomer conversion, in 2016, our group reported an alternative approach, which is RAFT dispersion copolymerization of St and MMA for reducing T_g of the formed diblock copolymer in the polymerization media, favorable to the polymerization in the nano-objects.[136]

Zhang *et al.* reported a new PISA formulation employing poly(ethylene glycol) (PEG) with a molecular weight ranging from 200 to 1000 Da as the polymerization medium in RAFT dispersion polymerization.[132] Accelerated RAFT polymerization was observed due to the compartmentalization effect or radical segregation compared to conventional alcoholic dispersion RAFT polymerization. In the viscous PEG polymerization medium, new morphologies of the ellipsoidal vesicles and the nanotubes were formed. Recently, Armes *et al.* reported the preparation of poly(stearyl methacrylate)–poly (benzyl methacrylate) (PSMA–PBzMA) diblock copolymer vesicles *via* RAFT dispersion polymerization in mineral oil.[137] In this nonpolar solvent, the vesicle-to-worm transition occurred when heating to 150 °C due to increased degree of solvation of

the solvophobic PBzMA blocks, reducing the packing parameter for the copolymer chains. Moreover, rheological results indicated that the inter-worm entanglements lead to the formation of gels, thus increasing solution viscosity. This unique oil-thickening mechanism provides prospects for the potential commercial application of PISA-generated materials.

2.1.2. Water. In contrast to organic solvents used for PISA, water is a green, economical and abundant solvent, thus aqueous RAFT dispersion polymerizations have attracted considerable research attention. An important prerequisite for aqueous dispersion polymerization is that a water-miscible monomer generates a water-insoluble polymer by polymerization. In 2011, Armes *et al.* pioneered the monitoring of morphology evolution from spheres to worms to vesicles in RAFT aqueous dispersion polymerization of 2-hydroxypropyl methacrylate (HPMA) with poly(glycerol methacrylate) (PGMA) as macro-CTA.[138] In this study, they observed that spherical micelles were formed initially, and then various morphologies including worms, octopi, jellyfish and vesicles were formed through the morphological transitions, the same as alcoholic RAFT dispersion polymerization.

As aforementioned, the normal transition sequence in the PISA is the spheres-to-nanorods-to-vesicles transition. Recent studies revealed that the interactions of the monomer or the additive molecules, such as dynamic covalent and host–guest interactions, affected the morphology transitions. In the preparation of PGMA–PHPMA diblock copolymer vesicles, Armes *et al.* observed a vesicle-to-worm/sphere morphological transition because a specific binding of 3-aminophenylboronic acid (APBA) with the pendent *cis*-diol groups of the hydrophilic PGMA block increased the effective volume, resulting in the reduction of the packing parameter (Fig. 1A).[139] Yuan *et al.* reported an interesting example of the direct preparation of nanotubes by the utilization of a cyclodextrin/styrene (CD/St) complex.[140] In this report, the spontaneous *in situ* self-assembly of amphiphilic PEG-*b*-PS diblock copolymers generated nanoparticles with various morphologies including spheres, worms, lamellae, and nanotubes (Fig. 1B). The complexation between the CD and the St limited the plasticizing degree of the PS block and reduced the mobility of PS chains, and thus kinetically trapped lamellae and nanotubes were preferred instead of conventional spherical vesicles. Notably, the produced nanoparticles still exhibited excellent stability after the removal of the free CDs. Moreover, the host/guest chemistry reported by Yuan provides a genius route for the aqueous dispersion polymerization of hydrophobic monomers.

Recently, Rieger *et al.* proposed a novel templated PISA strategy towards anisotropic morphologies.[141] A hydrogen-bonded bis-urea sticker was introduced to the macro-RAFT agent, which preorganized in fibre-like micelles. The chain-extended dispersion polymerization of 2-methoxyethyl acrylate (MEA) in water yielded long fibers through a templating mechanism, which was different from that of the conventional PISA system.

2.2. Photo-regulated RAFT polymerization

The above-mentioned PISA systems are mediated by RAFT polymerizations under thermal initiation and usually require a relatively high reaction temperature (above 60 °C), which is unfavorable for the preparation of temperature-sensitive nanomaterials because the high polymerization temperature can lead to the denaturation of proteins, antibodies, enzymes and other biologically active substances. The newly emerging photo-controlled living radical polymerization (photo-CRP) offered great opportunities due to its good control over polymerizations and the use of mild reaction conditions. Recently, significant advances have been made towards the fabrication of polymeric nanomaterials *via* PISA mediated by the photo-CRP method.[142–144]

In 2013, Tan *et al.* reported the first room-temperature photo-initiated RAFT dispersion polymerization under 365 nm irradiation for the preparation of highly monodisperse PMMA microspheres.[145] In this process, the macro-RAFT agent acted as a stabilizer and control reagent simultaneously, and besides, a small molecular RAFT agent, such as *S*-1-dodecyl-*S*′-

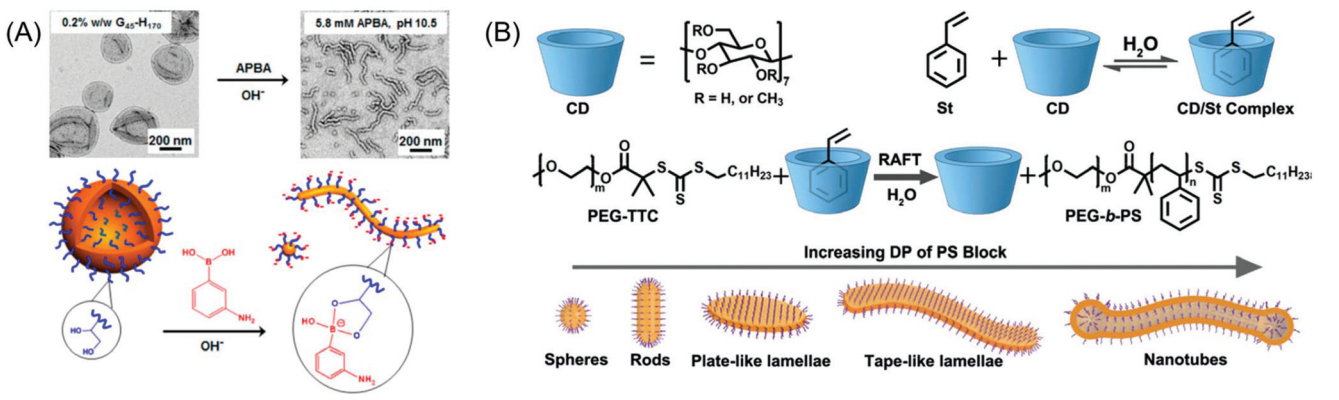

Fig. 1 (A) Schematic cartoon for vesicle-to-worm transition induced by the selective binding of APBA to the PGMA stabilizer chains. Reproduced from ref. 139 with permission from the American Chemical Society, copyright 2017. (B) Representation of RAFT dispersion polymerization of the CD/St complex in water. Reproduced from ref. 140 with permission from Wiley-VCH, copyright 2017.

(α,α′-dimethyl-α″-acetic acid) trithiocarbonate (DDMAT) was used to ensure the effective control of the polymerization.

Thanks to the success of visible light-initiated RAFT polymerization, the first example for the preparation of self-assembled nano-objects *via* the visible light-initiated PISA process (photo-PISA) was reported by Cai and co-workers in 2015.[146] In this initial work, sodium phenyl-2,4,6-trimethylbenzoylphosphinate (SPTP) was employed as a water-soluble photo-initiator in the chain extension of poly(2-hydroxypropyl methacrylamide) (PHPMAm) macro-CTA with diacetone acrylamide (DAA) under visible light irradiation, resulting in the simultaneous chain growth and *in situ* formation of spherical nanoparticles.

Later, this photo-PISA methodology was used to synthesize nanoparticles with more complex morphologies.[142,147–151] For example, Tan *et al.* reported the visible light-initiated PISA that formed the full range of morphologies (including spheres, worms, lamellae, unilamellar vesicles, jellyfish, branched worms, and multilamellar vesicles) at room temperature.[147] This work expended the scope of application of photo-PISA.

Inspired by the fact that some RAFT agents undergo photolytic cleavage of the C–S bond, leading to the formation of carbon centered radicals that can initiate polymerization,[152] therefore, an alternative approach, which was known as photoiniferter mechanism, was studied intensively by a number of groups, and they performed the RAFT dispersion polymerization without exogenous catalysts or initiators.[153–159] This technique demonstrated the formation of the various morphologies including spherical micelles, worms and vesicles *via* the PISA process. Despite the advantage of applicability to different solvent media, a shortcoming of this system lies in the relatively low polymerization rates compared to that reported with a photoinitiator or photocatalyst.

In 2014, Boyer and coworkers introduced the concept of photoinduced electron transfer-reversible addition–fragmentation chain transfer (PET-RAFT) polymerization, and demonstrated that the photocatalysts such as $Ir(ppy)_3$ and $[Ru(bpy)_3]Cl_2$ can be directly utilized in RAFT dispersion polymerization under visible light.[160,161] This technique is compatible with a wide range of monomers, including methacrylates, acrylates, styrene, acrylamides, methacrylamides and so on. Soon after, the same group demonstrated the first example of a PISA process based on PET-RAFT under visible light (λ = 460 nm, 0.7 mW cm^{-2}), and poly(oligo(ethylene glycol) methyl ether methacrylate) (POEGMA) was chain extended with BzMA to achieve *in situ* self-assembled polymeric nano-objects with different morphologies.[162] In this study, $[Ru(bpy)_3]Cl_2$ was employed to regulate the dispersion polymerization, and by strict manipulation of the reaction parameters, such as solid contents and the solvent, different nanoparticle morphologies varying from spherical micelles to vesicles were achieved. The "ON/OFF" control over the dispersion polymerization was confirmed, allowing for temporal control over the nano-object morphology. In these studies, a metal coordination complex was used as the photocatalyst and contamination of the polymer products might be a problem.

In 2017, our group reported an alternative PISA process for the preparation of nano-objects with different morphologies under metal free conditions.[163] In this study, instead of heavy-metal based photocatalysts, 10-phenylphenothiazine (PTH) was used to regulate the RAFT dispersion polymerization of BzMA, and ON/OFF control over the polymerization was also observed.

Despite the great advances in PET-RAFT mediated or photo-initiated PISA systems, the use of visible light or UV light also poses some challenges regarding the large-scale preparation of nanomaterials for potential commercial applications compared to the conventional thermally initiated systems. Specifically, the attenuation and poor penetration of light in the polymerization system and the nanoparticle-induced scattering during the polymerization will be more pronounced under heterogeneous conditions and scaled-up productions, which is unfavorable for the consistency of the obtained materials. One effective method to relieve the abovementioned limitation is the utilization of longer wavelengths of light in photo-PISA.[164] In 2017, Boyer *et al.* reported a PISA formulation conducted under long wavelength visible red light (λ_{max} = 635 nm) mediated by 5,10,15,20-tetraphenyl-21*H*,23*H*-porphine zinc (ZnTPP). By varying the DP for the hydrophobic block, nanoparticles with different morphologies including spheres, wormlike micelles, and vesicles were formed.[164] The use of a low energy wavelength could weaken nanoparticle-induced scattering and provide a favorable method for the incorporation of light-sensitive compounds during the PISA process.

More recently, an alternative approach by the application of the continuous flow technique in photo-PISA (Fig. 2) was reported by groups of Boyer and Tan.[165–167] By increasing the DP of the second block PBzMA, nano-assemblies with various morphologies varying from spheres, to worms and to vesicles were produced.[165]

2.3. Enzyme-initiated RAFT polymerization

In 2015, An *et al.* firstly reported enzyme-initiated RAFT polymerization using a horseradish peroxidase (HRP)/H_2O_2/acetylacetone (ACAC) ternary initiating system.[168] In this process, HRP catalysed the oxidation of ACAC using H_2O_2 to produce ACAC radicals (Fig. 3), which then initiated RAFT polymerization for the preparation of different types of the block copolymers in a controlled manner. The HRP-initiated RAFT polymerization can also be conducted under dispersion polymerization conditions, leading to the formation of block copolymer nanoparticles.

Tan and coworkers reported the synthesis of block copolymer nano-objects with complex morphologies including spheres, worms, and vesicles *via* enzyme-PISA under mild conditions.[149,169] In a recent study, with the catalyst of HRP, RAFT-mediated PISA was performed under ambient temperature and a full range of morphologies were obtained.[169] By monitoring the viscosity of the reaction system, they prepared pure worm-like nano-objects. Another application of enzymes in PISA is the combination of the enzyme catalytic reaction

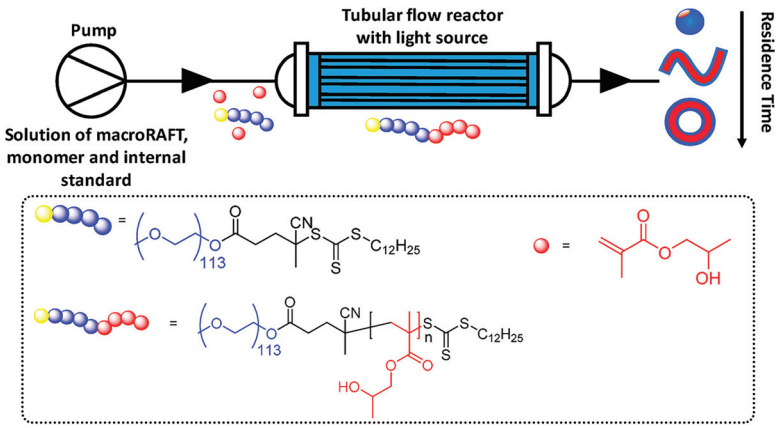

Fig. 2 RAFT-mediated photo-PISA syntheses performed under continuous flow conditions. Reproduced from ref. 166 with permission from the American Chemical Society, copyright 2018.

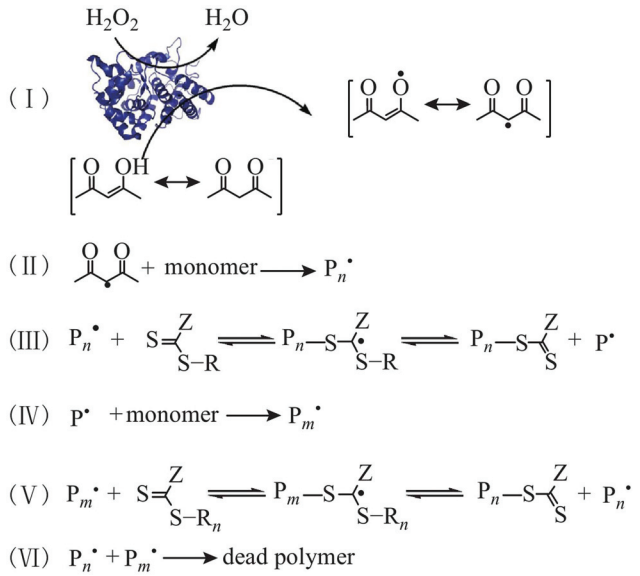

Fig. 3 Mechanism of HRP-initiated RAFT polymerization. Reproduced from ref. 168 with permission from the American Chemical Society, copyright 2015.

with the photo-PISA to realize oxygen tolerant and high-throughput PISA, which is of great significance to study the mechanism of morphology transformation and extend the application of PISA.[23,149,169,170]

3. Atom transfer radical polymerization (ATRP)

ATRP is one of the most widely used living polymerization method for the preparation of polymers with various architectures and composition; however, only a few articles have been reported that use ATRP in the PISA process.[77–80,82–91] One major barrier for the application of the ATRP in PISA is the difficulty in the purification of the final products due to the use of the copper catalyst or transition metal catalyst. In order to extract the residual copper catalyst in the polymer products, dialysis and the copolymerization of a cross-linker are the most adopted strategies. In 2007, our group studied the atom transfer radical dispersion polymerization (ATRDP) of 4-vinylpyridine (4VP) in an ethanol/H_2O mixture using PEG-Br as the both initiator and stabilizer. Stabilized spheres were successfully prepared by the copolymerization of 4VP with the crosslinker *N*,*N*′-methylenebisacrylamide (MBA).[78] Armes *et al.* synthesized shell cross-linked (SCL) micelle based PEO–poly(dimethylamino)ethyl methacrylate (PDMA)–poly(2-(methacryloyloxy)ethyl phosphorylcholine) (PMPC) triblock copolymers using ATRP. The cross-linking reaction in this system was achieved *via* the quaternization reaction of the DMA residues with 1,2-bis(2-iodoethoxy) ethane (BIEE).[79] Another problem caused by the metal catalyst in ATRP is the difficulty in controlling the location of the transition metal catalyst during dispersion/emulsion polymerization.[31] With the developments of the improved ATRP procedures, which featured lower concentration of the catalyst (ppm) and higher tolerance to impurities and air, considerable efforts have been devoted to enriching the versatility of the ATRP PISA technique. These ATRP procedures include reverse ATRP, simultaneous reverse and normal initiation (SR&NI) ATRP,[171] activator generated by electron transfer (AGET) ATRP,[172,173] initiators for continuous activator regeneration (ICAR)ATRP,[174] activators regenerated by electron-transfer (ARGET)ATRP,[175] supplemental activators and reducing agent (SARA)ATRP,[176] and so on. Among the abovementioned improved ATRP techniques, the ICAR ATRP can be conducted at a low ppm of copper catalyst concentration, and has been proved to be a powerful tool to prepare nano-objects by PISA.

In 2016, Matyjaszewski and coworkers reported the fabrication of various nano-objects including spheres, wormlike aggregates, and vesicles by ICAR ATRP PISA (Fig. 4). Poly(oligo (ethylene oxide) methyl ether methacrylate) (POEOMA) was synthesized at first and used as the macroinitiator and stabilizer. In the PISA process, BnMA was adopted as the second monomer, tris(pyridin-2-ylmethyl)amine (TPMA)/$Cu^{II}Br_2$ was

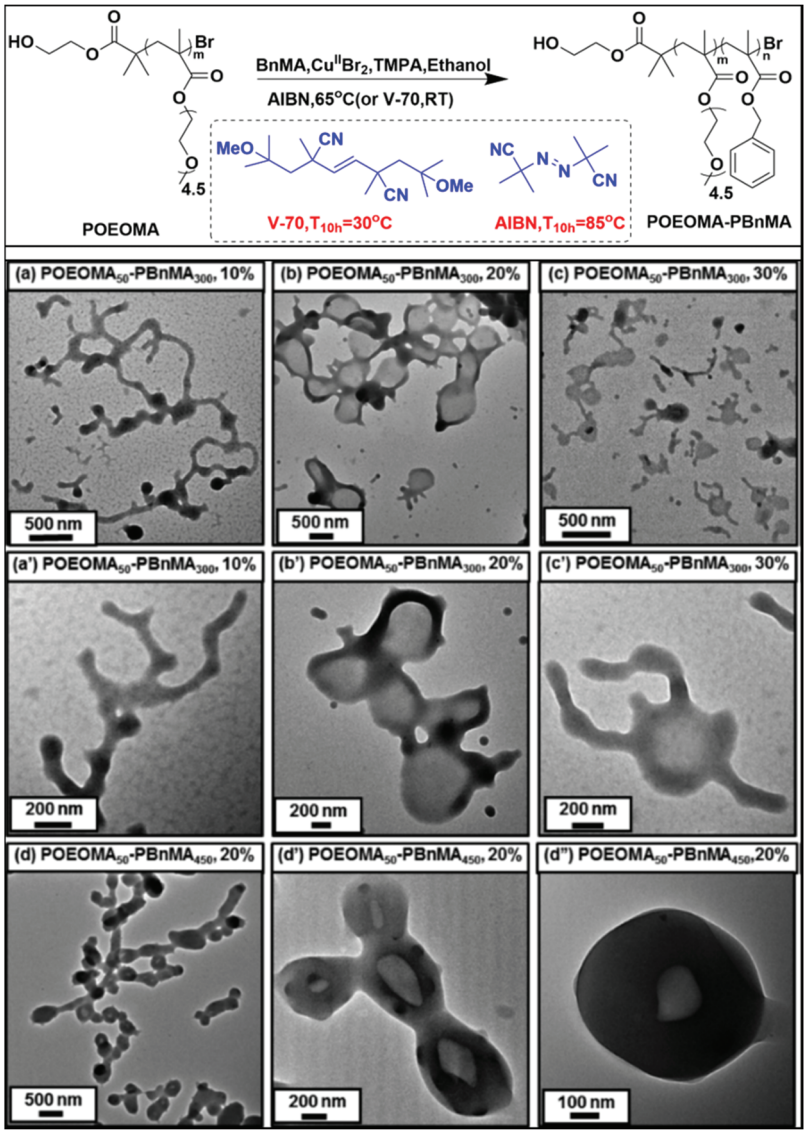

Fig. 4 Polymerization-induced self-assembly (PISA) using ICAR ATRP at a low catalyst concentration. Reproduced from ref. 83 with permission from the American Chemical Society, copyright 2016.

chosen as the catalytic system. To achieve controllable polymerization under a low ppm of copper catalyst concentration, PISA was conducted at 65 °C, when $[Cu^{II}Br_2]_0$ was set as 400 ppm, and the ICAR ATRP PISA proceeded in a controlled manner.[83]

Recently, Zhang *et al.* reported the synthesis of diblock copolymer nano-objects by PISA under ICAR ATRP and RAFT dispersion polymerization and compared the difference in the morphologies.[86,88] They synthesized PEG-*b*-PS nano-objects by ATRP using a PEG-Br macroinitiator in the presence of $CuBr_2$/tris(2-pyridylmethyl)amine, and the obtained nano-objects were compared with those synthesized *via* traditional RAFT dispersion polymerization under similar conditions. It was found that the morphologies of nano-objects prepared by ATRP were more complicated. Detailed comparative experiments revealed that the morphological difference was attributed to the high $Đ$ of the obtained BCPs and the use of the copper catalyst in ICAR ATRP dispersion polymerization.

4. Ring-opening metathesis polymerization (ROMP)

Different from the conventional living radical polymerization (LRP), ROMP is a nonradical methodology to prepare nano-objects of various morphologies.[99–117] It is worth mentioning that in a recent review, O'Reilly *et al.* systematically introduced the applications of ROMP in PISA processes, covering the general concepts of the ROMPISA strategy.[101] Here we briefly summarize some relevant work. The concept of *in situ* preparation of block copolymer nano-objects *via* ROMPISA in toluene was initially introduced by Xie and coworkers.[99] In this

study, poly(2,3-bis(2-bromoisobutyryloxymethyl)-5-norbornene) (PBNBE) was synthesized with the $(PCy_3)_2(Cl)_2Ru{=}CHPh$ (G1) catalyst at first, and then used as a macroinitiator in the subsequent chain-extension of the oxanorbornene dicarboxylic acid dimethyl ester (ONBDM) monomer. The block copolymers self-assembled into spherical micelles composed of a densely packed core of the PONBDM blocks and the shell of PBNBE blocks through PISA process. Soon after, following this one-pot ROMPISA procedure, by using the same PBNBE macroinitiator, they extend this method to fabricate functional polymeric nanoparticles with UV-cross-linkable cores *via* copolymerization of a cinnamyl-based ONB monomer and ONBDM in toluene. The core-cross-linked micelles were obtained after UV irradiation.[100] In 2012, Choi's group reported a direct one-pot route for the preparation of self-assembled nanostructures directly from polyacetylene diblock copolymers, which were synthesized *via* ROMP of cyclooctatetraene (COT) using polynorbornene (PNB) as the macroinitiator and $(H_2IMes)(py)_2(Cl)_2Ru{=}CHPh$ (G3) as the catalyst.[102] Inspired by the observation that liquid NMR spectroscopy showed signals only for the solvophilic polynorbornene block, they investigated the self-assembly behavior of PNB-*b*-PA (PA: polyacetylene). As the insoluble PA block lengthened, the morphologies changed from nanospheres to wormlike micelles (nanocaterpillar structure), and the ratio of the populations of the wormlike and spherical micelles increased as the amount of COT increased, which was attributed to strong π–π interactions of exposed PA cores between adjacent nanospheres, favouring the minimization of the area of solvophobic PA cores. It is worth mentioning that at least more than 10% of the nanospheres failed to transform into nanocaterpillars in this report, due to the existence of stereo-random polyenes and broad molar mass dispersity of the PA blocks. In follow-up work, by altering the ROMP temperature, control over the stereochemistry (E/Z) of the PA block, the degree of chain-transfer reaction and molar mass dispersity was achieved by Choi and coworkers, as a result, defect-free nanocaterpillars were successfully prepared.[103]

Compared to the above-mentioned examples about ROMPISA in organic media, water is a green and abundant solvent, however, aqueous ROMPISA has only very recently emerged and was less reported. One major barrier is that conventional Ru-catalyzed olefin metathesis is commonly conducted in dry and anhydrous organic solvent under inert atmosphere, and water must be rigorously excluded as it would lead to the probable deactivation of the catalyst. Some recent progress has been made in addressing this problem by exploitation of water-soluble ruthenium catalyst.

In 2018, Gianneschi *et al.* demonstrated the utilization of an aqueous quaternary amine Hoveyda–Grubbs 2nd generation initiator for the preparation of poly(oligo ethylene glycol) (POEG)-*b*-poly(quaternary amine phenyl norbornene) block copolymer particles *via* one-pot aqueous ROMPISA under a nitrogen atmosphere (Fig. 5A). The hydrophilic macroinitiator was synthesized using the solution ROMP of OEG, and subsequent chain-extension was achieved upon continuous charging of the quaternary amine phenyl NB dicarboximide under identical polymerization conditions for the formation of the hydrophobic core. By varying the POEG block length, a range of well-defined nanostructures, including spherical micelles, worms and vesicles, were prepared *in situ*.[112] In later studies, Gianneschi's group extended this one-pot aqueous ROMPISA methodology to fabricate different functional nano-objects, such as enzyme-responsive and pH-responsive nano-objects.[116,117]

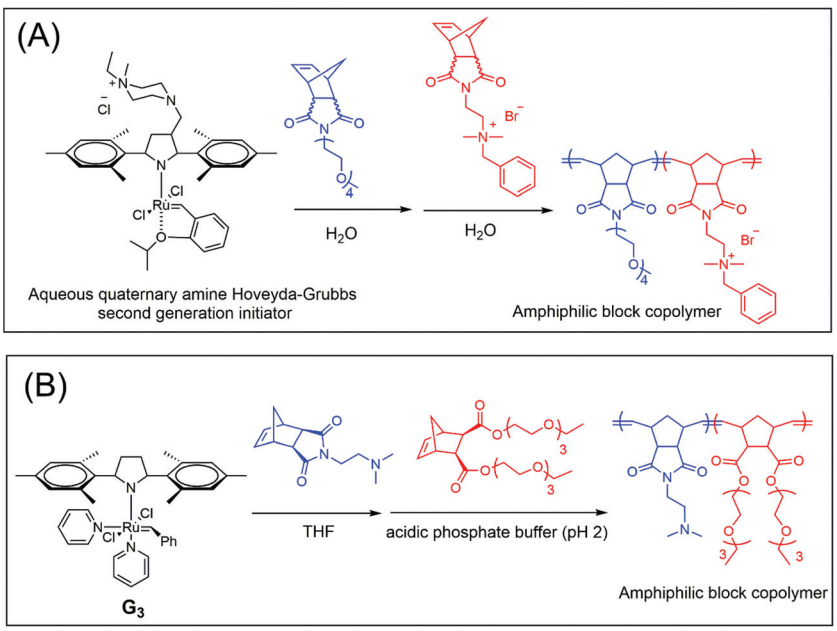

Fig. 5 (A) Aqueous ROMPISA mediated by a water-soluble ruthenium initiator. Reproduced from ref. 112 with permission from the American Chemical Society, copyright 2018. (B) Aqueous ROMPISA by preparation of a water-soluble macroinitiator in organic solvent which mediates living ROMP in aqueous milieu. Reproduced from ref. 111 with permission from Wiley-VCH, copyright 2018.

Recently, O'Reilly's group introduced a general strategy for ROMPISA in aqueous milieu,[111,115] which relied on the prior preparation of a water-soluble macroinitiator in organic solvent. In their initial report,[111] a hydrophilic PNB macroinitiator was synthesized in THF using a commercially available G3 catalyst, which was then transferred to an acidic solution (pH = 2) of core-forming monomers for the ROMPISA process, and the nano-objects with various morphologies (Fig. 5B), such as spheres, worms and vesicles were *in situ* fabricated. This two-step aqueous ROMPISA methodology prevents the issue of slow initiation in H_2O, and the polymerization proceeded in a fast and controlled manner; the resulting polymers featured narrow molecular weight distributions.

Cunningham and coworkers reported an alternative approach to prepare diblock copolymer nano-objects by one-pot aqueous ROMPISA under emulsion polymerization conditions.[114] In the first step, a PEG-functionalized norbornene (NB-PEG) was polymerized in water initiated by a water-soluble PEGylated G3 catalyst under inert atmosphere at room temperature, and then water-immiscible monomer 1,5-cyclooctadiene (COD) was added into the system, continuing the emulsion polymerization. It was observed that a higher ratio of NB-PEG could decrease the particle size, which might be attributable to particle stabilization by PEG groups. By varying the concentrations of hydrophilic versus hydrophobic monomer (30 mol% of NB-PEG and 70 mol% of COD), stable latexes with final particles of ≈200 nm diameter were obtained.

Conventional PISA generally employs reversible deactivation radical polymerization (RDRP) as the chain-extension mechanism because it allows for a wide range of functional monomer families and solvents. However, it shows poor tolerance to some functionalities such as alkyne, thiol, and stable radicals. ROMP is an attractive alternative route for conducting PISA to prepare nanoparticles with specific functionalities. Recently, Delaittre and coworkers reported a tandem ROMP-ROMPISA methodology for the synthesis of nitroxide-functionalized polymer nanoparticles.[113] The nitroxide-functionalized solvophilic precursor was synthesized by ROMP of oligoethylene glycol-modified norbornene (NOEG) and TEMPO-functionalized norbornene monomer (NTEMPO) with first-generation Grubbs catalyst (G1). Subsequently, the solution of norbornene in ethanol was injected for the chain extension leading simultaneously to the formation of nanoparticles. The obtained TEMPO-functionalized NPCs show excellent catalytic activity and recycling capacity for the oxidation of alcohols. Besides, they exhibit antioxidant activity and no *in vitro* toxicity, suggesting the potential of this ROMPISA methodology to produce antioxidant or MRI imaging agents.

5. Nitroxide-mediated living free-radical polymerizations (NMP)

In 2009, Charleux's group reported the fabrication of complex morphologies employing one-step nitroxide-mediated emulsion polymerization.[45] In this study, water-soluble SG1-terminated

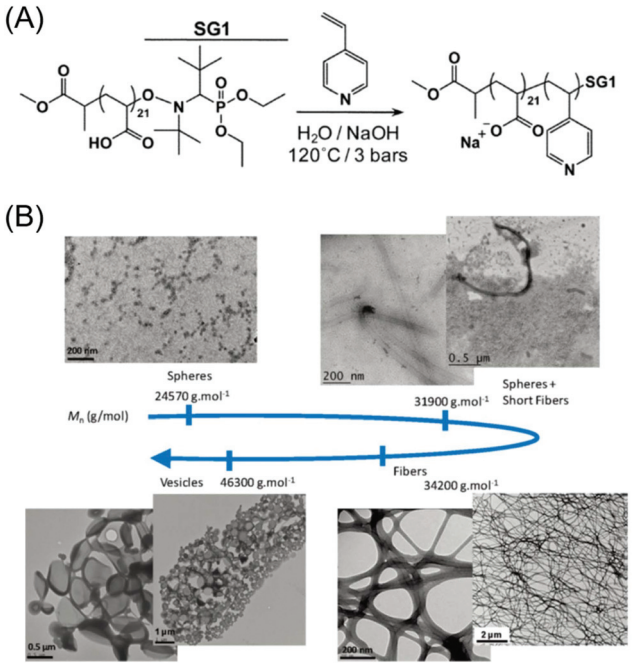

Fig. 6 (A) NMP of 4VP initiated by poly(sodium acrylate)–SG1 macroalkoxyamine. Reproduced from ref. 45 with permission from the Royal Society of Chemistry, copyright 2009. (B) TEM images of various nano-objects obtained with different hydrophobic block lengths. Reproduced from ref. 68 with permission from the American Chemical Society, copyright 2012.

(SG1: *N-tert*-butyl-*N*-[1-diethylphosphono(2,2-dimethylpropyl)] nitroxide, Fig. 6A) poly(sodium acrylate) was used as the macroinitiator, which was synthesized by the SG1-mediated polymerization of acrylic acid.[177] In order to ensure the solubility of the macroalkoxyamine and stability of SG1, the polymerization process of the core-forming monomer 4VP was conducted at pH = 11. The simultaneous chain-extension and self-assembly led to the formation of various particle morphologies, such as wormlike micelles, spherical vesicles, elongated vesicles and multicompartmented vesicles. Due to the existence of the pH-sensitive P4VP block, when the pH of the suspension was decreased to 2, the protonation of the P4VP block led to the dissociation of the formed self-assembled nano-objects. However, rebasification of the medium to pH 12 did not lead to the reformation of the initial morphologies, but instead classical core–shell spherical micelles, demonstrating the formation of out-of-equilibrium structures during the PISA process.

Later, the same group realized the production of well-defined morphologies *via* fine-tuning of the block lengths.[68] The emulsion polymerizations of MMA with a small portion of St were carried out in the presence of NaOH (pH ~ 7) and different concentrations of P(MAA-*co*-SS)-SG1 (methacrylic acid, MAA, and sodium 4-styrene sulfonate, SS) so as to target different lengths of the hydrophobic blocks. For a given length of the hydrophilic block, the increase in the chain length of the hydrophobic block led to morphology evolution from spheres to nanofibers to vesicles (Fig. 6B).

Bourgeat-Lami *et al.* investigated PISA in aqueous emulsion using brush-type macroalkoxyamines entirely composed of PEOMA (poly(ethylene oxide)methyl ether methacrylate) macromonomer units.[71] In the emulsion polymerization of *n*-butyl methacrylate, a low percentage (<10 mol%) of styrene was added as a comonomer to enhance the reversible deactivation process and to lead to stable alkoxyamines. Surprisingly, the self-assembled diblock copolymer particle morphologies could change from spherical micelles to vesicles when the pH was increased from 4.2 to 6.7, even when the macroalkoxyamine initiator contained only one terminal methacrylic acid unit. Furthermore, the particle morphologies could be tuned from spherical to elongated micelles and vesicles by the addition of increasing amounts of NaCl at pH ~4.2. These results suggest a salting out effect produced by the increase of ionic strength, which is an alternative way to control the particle morphology during the PISA process independent of regulating the length of the hydrophilic and hydrophobic blocks. Recently, they reported the first example of utilizing the NMPISA in the synthesis of organic/inorganic particles.[74] A brush-like PEOMA-based macroalkoxyamine initiator was synthesized and adsorbed on the surface of silica particles, and further emulsion polymerization of *n*-butyl methacrylate and styrene led to the formation of silica/polymer particles with different morphologies. By varying experimental conditions, such as the silica particle size and macroinitiator concentration, silica/polymer hybrid particles with dumbbell-, raspberry-, and daisy-shaped morphologies were successfully prepared. Later, they investigated the effect of pH on this surface-PISA process, and the silica/polymer latexes with some unconventional morphologies such as concentric core–shell–corona, half-capped, snowman-like vesicular, tadpole- and centipede-like morphologies have been produced.[76]

NMPISA can also be conducted under dispersion polymerization conditions.[66,69] Charleux *et al.* demonstrated the synthesis of thermoresponsive nano-objects using PAA-SG1 macroinitiators for the dispersion polymerization of *N*,*N*-diethylacrylamide (DEAAm), which is a water-soluble monomer and the homopolymer PDEAAm exhibits an LCST (lower critical solution temperature) of approximately 32 °C. Thus, the obtained nanoparticles with the PDEAAm core were thermoresponsive. Consequently, at room temperature, the latex turned into a homogeneous solution of water-soluble diblock copolymers. Upon heating of this solution above the critical temperature, nanoparticles reformed but with dimensions significantly larger than the initial ones, proving once again the formation of out-of-equilibrium nanostructures during the PISA process. When *N*,*N*′-methylenebis-(acrylamide) (MBAAm) was introduced as a cross-linker in the dispersion polymerization reaction, crosslinked particles or nanogels formed under different concentrations of the cross-linker.

6. Ring-opening polymerization (ROP) of *N*-carboxyanhydride (NCA)

Examples of PISA utilizing ROP are scarce. Recently, Du's group reported the first case of PISA based on the ROP of α-amino acid NCAs of L-phenylalanine monomers (L-Phe NCAs) which was initiated by methoxypolyethylene glycol amine (PEG-NH_2) in tetrahydrofuran (Fig. 7A).[178] With the DP increase of the PPhe block, their solubility in THF is constantly reduced, resulting in the phase separation. The morphologies

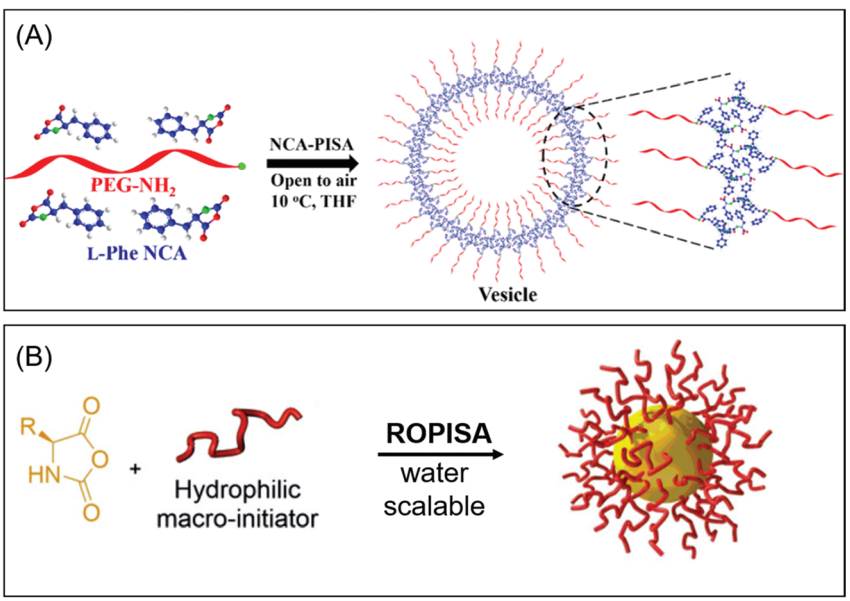

Fig. 7 (A) Biodegradable polymer vesicles by NCA-PISA. Reproduced from ref. 178 with permission from the American Chemical Society, copyright 2019. (B) One-step approach by ring-opening polymerization induced self-assembly (ROPISA). Reproduced from ref. 179 with permission from Wiley-VCH, copyright 2019.

of the nano-objects can be regulated upon varying the target DP of the core-forming block and the solid content, different nanoparticle morphologies such as spherical micelles and hollow vesicles were successfully prepared. Interestingly, during the NCA-PISA process, a nearly constant rate of polymerization was observed due to the excellent solubility of monomers in THF, which was different from conventional ROP. The *in vitro* biodegradability experiments indicated that the NCA-PISA-generated vesicles had good biodegradability. Furthermore, this methodology is extendable to other NCA monomers, for example, L-aspartic acid β-benzyl ester.

In the conventional ROP process, water must be rigorously excluded as it would lead to the hydrolysis and uncontrolled polymerization of NCA. In a recent study, Bonduelle and coworkers demonstrated the first example of self-assembled nanostructures *via* ROPISA in aqueous media (Fig. 7B).[179] They utilized a hydrophilic α-amino-poly(ethylene glycol) (PEG-NH_2) as the initiator, and the subsequent aqueous ROP process of γ-benzyl-L-glutamate *N*-carboxyanhydrides (BLG-NCA) was conducted under pH = 8.5, because NCA aminolysis is greatly limited at this pH value. Besides, the micelles formed by the short diblock of PEG-*b*-PBLG at the early stage of the polymerization can also protect the unpolymerized NCA monomers from hydrolysis. The obtained amphiphilic PEG-*b*-PBLG diblock copolymers featured narrow dispersity, and by judicious selection of the initiator to monomer ratio and the solid content, the copolymers could self-assemble into various nanostructures, for example, needle and worm-like morphologies. It is worth mentioning that the ROPISA process of NCA monomers was strongly influenced by the secondary structure of the polypeptides which is a unique feature of this PISA process.

7. Living anionic polymerization (LAP)

Before the PISA concept was proposed, pioneering studies by Murray *et al.*, Okay *et al.* and Kim *et al.* exploited anionic dispersion polymerization of styrene (St) or divinylbenzene in *n*-hexane in the presence of a poly(*t*-butyl styryl)-lithium or polyisoprenyllithium macroinitiator, and indeed probably involved the self-assembly of block copolymers during polymerization.[180–182] More recently, one representative example of PISA based on LAP is lithium-initiated living anionic polymerization of butadiene (BD) and styrene in hexane by the sequential addition of first BD and then styrene after all the BD was completely polymerized.[94] The self-assembly process occurred due to the solubility difference between the two blocks: the PS block is significantly insoluble in hexane whereas the PBD block is very soluble in this solvent. Spherical micelles with a PS core and PBD shell were formed when the chain length of PS blocks reached the critical micelle degree of polymerization (CMDP). Apart from the spherical micelles, hollow nanoparticles were also prepared with the well-designed one-pot and two-step method. The nanosized PS globules were elaborately utilized to produce the removable core during the micellization of PBD-*b*-PS diblock copolymers. Another interesting approach was also designed by using a mixture of di- and tri-block copolymer initiators in the micelle formation process. By varying the ratio of triblock to diblock copolymers as well as the molecular weight of the centered PBD block in the triblock copolymer, non-spherical particles varying in shape from ellipsoids to cylinders and long linear or branched strings were formed.

Hashimoto *et al.* reported the first utilization of real-time small-angle neutron scattering (SANS) to directly observe the PISA process which occurred in the LAP of isoprene (I) and styrene-d_8 (St).[92,93,95] The polymerization of I and St in benzene-d_6 was conducted in one-pot. The great disparity in the reactivity between these two monomers promoted the polymerization to produce a PI-*b*-PS diblock copolymer. The structural changes during the polymerization process were induced only by self-assembly of the growing chains. The polymerization-induced disorder–order transition from the disorder state to the cylindrical microdomain structure and order–order transition from cylindrical to lamellar structure were first observed indirectly by time-resolved SANS analysis.

In 2017, combining PISA and crystallization-driven self-assembly (CDSA) protocols, Manners and coworkers introduced a renewed utilization of LAP to produce non-spherical micelles, which was termed PI-CDSA.[98] Anion-terminated polyisoprene (PIP) was prepared by LAP in THF, and was then transferred to a solution of dimethylsila[1]ferrocenophane (FDMS) monomer in a mixture of dry THF/*n*-hexanes. The polymerization and self-assembly occurred almost simultaneously throughout the PI-CDSA process, leading to the formation of non-spherical particles varying in shape from platelet to cylindrical under the stringent conditions (such as solid content and block ratio) driven by crystallization of the structure-directing PFDMS block. This PI CDSA process enables CDSA to be performed at much higher concentrations than that previously achieved. Moreover, this method achieves living length control over the obtained nanowires, which is difficult for established PISA techniques.

Most recently, Wang *et al.* reported the LAP PISA process to construct nano-objects from styrenic copolymers.[183] In this study, an all-styrenic diblock copolymer poly(*p*-*tert*-butylstyrene)-*b*-polystyrene (P*t*BS-*b*-PS) was synthesized in heptane and used as a model example to systematically investigate the PISA formulation. By modulating the length and length ratio of the PtBS and PS blocks and solid content, nano-objects of different morphologies that varied from spherical micelles to vesicles were generated (Fig. 8), and the phase diagram was depicted.

8. Organotellurium-mediated radical polymerization (TERP)

It is well known that different types of monomers in the presence of organic tellurium compounds as the control agents

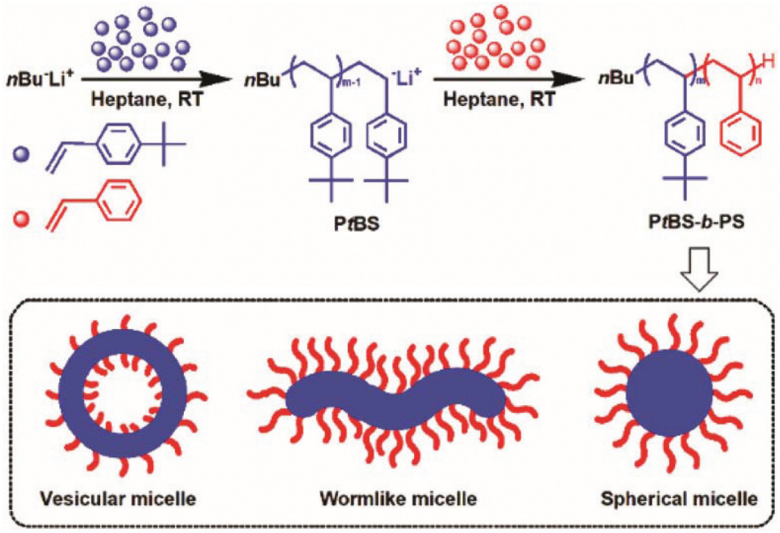

Fig. 8 The illustration of the LAP PISA process based on the all styrenic diblock copolymer PtBS-*b*-PS. Reproduced from ref. 183 with permission from the Royal Society of Chemistry, copyright 2020.

can undergo organotellurium mediated controlled/"living" radical polymerization (TERP). Okubo's group applied the TERP in PISA,[184–189] and they used poly(methacrylic acid)-methyltellanyl (PMAA-$TeCH_3$) as a macro-CTA in emulsion polymerizations of styrene and *n*BA. They found that a high stirring rate of the polymerization system had a favourable influence on the particle size distribution and the livingness of the polymerization due to the lower viscosity inside polymerizing particles and higher consumption of the control agent. Well-defined PMAA-based block copolymer spherical particles of a small size (D < 50 nm) were indeed obtained at a stirring rate of 1000 rpm, while a slow stirring rate (220 rpm) led to the formation of broad, bimodal spheres with nanometer- and submicrometer-sized distributions.[184,188] In the emulsion polymerization process, another factor, which should be considered, was the particle formation mechanisms. A lower polymerization temperature was a key point to avoid homogeneous nucleation, and was favourable to self-assembly nucleation, and the latter is important for the formation of monomodal nanometer-sized particles.[187,188] Later, Okubo and coworkers synthesized PMMA particles with a narrow distribution with good colloidal stability *via* emulsion TERP using the same PMAA-$TeCH_3$ macro-CTA, with the $(TeMe)_2$ catalyst.[189] Because $(TeMe)_2$ had a certain solubility in water, it could work well as a catalyst in the aqueous phase, favouring the self-assembly nucleation.

9. Iodine-mediated polymerization (IMP)

In 2018, Goto and coworkers realized a heavy-metal-free and sulfur-free synthesis of poly (methacrylic acid)-*b*-poly(methyl methacrylate) (PMAA-*b*-PMMA) diblock copolymer using NaI catalyzed reversible complexation mediated living radical polymerization (RCMP), and then they successfully applied this polymerization technique in PISA.[190] Iodide-terminated PMAA-I was prepared at first and used as hydrophilic macroinitiators. In the following PISA process, MMA was chosen as a hydrophobic monomer and ethanol as the solvent. Varying the DPs of the PMAA-I and PMMA segments and the solid content led to the generation of different morphologies including micelles, worms and vesicles.

Recently, Zhu's group developed a photo-PISA methodology by combining the photo-controlled bromine–iodine transformation methodology with PISA to prepare nano-objects,[191,192] they investigated some factors that influenced the morphologies of the obtained nano-objects in detail. What is worth mentioning is that in these studies, the initiating dormant species alkyl iodides were produced *via in situ* nucleophilic substitution from alkyl bromines with NaI under irradiation with LED light.

10. Summary and outlook

In recent years, polymerization-induced self-assembly has been demonstrated to be a quite simple and efficient tool to produce amphiphilic block copolymer nano-objects with various morphologies in high concentrations. By taking advantage of the compatibility of various polymerization techniques, PISA is applicable to a wide range of monomer families and can be performed under different experimental conditions. Beyond polymerization techniques mentioned in this paper, other polymerization processes have also been utilized for PISA syntheses, including non-controlled polymerization.[193,194] In a recently published paper, Wan *et al.* reported the synthesis of rigid conjugated block copoly(phenylacetylene)s assemblies through coordination PISA.[195] The efforts for the

exploration of other controlled/"living" polymerizations continue to broaden the application scope of PISA, enabling the design and application of nanomaterials with various available monomers under different conditions.

Due to the tolerance to a broad range of reaction conditions and monomer families, RAFT polymerization is the predominantly used technique in PISA to date, where photo-regulated PISA can be conducted under mild reaction conditions (at room temperature), which is favourable for the preparation/loading of bioactive reagents. The other polymerization methods complement RAFT polymerization, for example, ROMP is an attractive alternative route for conducting PISA to prepare nanoparticles with specific functionalities, including alkyne, thiol, and radical. The ROPISA of NCAs lays a foundation for the efficient preparation of biocompatible and biodegradable nanomaterials.

Apart from the introduction of various polymerization processes, various approaches have been developed to broaden the PISA field, including the introduction of the new mechanisms such as polymerization-induced electrostatic self-assembly (PIESA), polymerization-induced crystallization-driven self-assembly (PI CDSA), and utilization of engineering approaches (continuous flow technique). We believe that the continuous progress of PISA will promote its development and the applications of PISA-generated materials.

Conflicts of interest

The authors declare no conflict of interest.

Note added after first publication

This review article replaces the version first published on 11th May 2020, which contained unattributed text overlap with a ChemComm highlight article, published by O'Reilly *et al.*, that was not cited in the original version. The review article has been rewritten and a citation has been added to the highlight article as ref. 101.

Acknowledgements

This work was supported by the National Science Foundation of China (No. 21525420 and 21774113).

References

1 B. M. Discher, Y.-Y. Won, D. S. Ege, J. C. Lee, F. S. Bates, D. E. Discher and D. A. Hammer, *Science*, 1999, **284**, 1143–1146.
2 Y. Y. Won, H. T. Davis and F. S. J. Bates, *Science*, 1999, **283**, 960–963.
3 D. E. Discher and A. J. Eisenberg, *Science*, 2002, **297**, 967–973.
4 J. B. Gilroy, T. Gädt, G. R. Whittell, L. Chabanne, J. M. Mitchels, R. M. Richardson, M. A. Winnik and I. J. Manners, *Nat. Chem.*, 2010, **2**, 566.
5 Y. Mai and A. J. Eisenberg, *Chem. Soc. Rev.*, 2012, **41**, 5969–5985.
6 S. G. Jang, D. J. Audus, D. Klinger, D. V. Krogstad, B. J. Kim, A. Cameron, S. W. Kim, K. T. Delaney, S. M. Hur and K. L. Killops, *J. Am. Chem. Soc.*, 2013, **135**, 6649–6657.
7 Z. Wang, M. C. van Oers, F. P. Rutjes and J. C. van Hest, *Angew. Chem., Int. Ed.*, 2012, **51**, 10746–10750.
8 I. Louzao and J. C. van Hest, *Biomacromolecules*, 2013, **14**, 2364–2372.
9 T. Liu, J. Hu, Z. Jin, F. Jin and S. Liu, *Adv. Healthcare Mater.*, 2013, **2**, 1576–1581.
10 Y. Y. Kim, K. Ganesan, P. Yang, A. N. Kulak, S. Borukhin, S. Pechook, L. Ribeiro, R. Kroger, S. J. Eichhorn, S. P. Armes, B. Pokroy and F. C. Meldrum, *Nat. Mater.*, 2011, **10**, 890–896.
11 H. Tian, J. Qin, D. Hou, Q. Li, C. Li, Z. S. Wu and Y. Mai, *Angew. Chem.*, 2019, **58**, 10173–10178.
12 L. Zhang and A. J. Eisenberg, *Science*, 1995, **268**, 1728–1731.
13 H. Shen, L. Zhang and A. J. Eisenberg, *J. Phys. Chem. B*, 1997, **101**, 4697–4708.
14 L. Zhang, H. Shen and A. Eisenberg, *Macromolecules*, 1997, **30**, 1001–1011.
15 F. Liu and A. J. Eisenberg, *J. Am. Chem. Soc.*, 2003, **125**, 15059–15064.
16 C. J. Ferguson, R. J. Hughes, B. T. T. Pham, B. S. Hawkett, R. G. Gilbert, A. K. Serelis and C. H. Such, *Macromolecules*, 2002, **35**, 9243–9245.
17 J. Rieger, W. Zhang, F. O. Stoffelbach and B. Charleux, *Macromolecules*, 2010, **43**, 6302–6310.
18 W. Zhang, F. D'Agosto, O. Boyron, J. Rieger and B. Charleux, *Macromolecules*, 2011, **44**, 7584–7593.
19 I. Chaduc, A. Crepet, O. Boyron, B. Charleux, F. D'Agosto and M. Lansalot, *Macromolecules*, 2013, **46**, 6013–6023.
20 V. J. Cunningham, A. M. Alswieleh, K. L. Thompson, M. Williams, G. J. Leggett, S. P. Armes and O. M. Musa, *Macromolecules*, 2014, **47**, 5613–5623.
21 N. P. Truong, M. V. Dussert, M. R. Whittaker, J. F. Quinn and T. P. Davis, *Polym. Chem.*, 2015, **6**, 3865–3874.
22 X. Dai, L. Yu, Y. Zhang, L. Zhang and J. Tan, *Macromolecules*, 2019, **52**, 7468–7476.
23 J. Tan, X. Dai, Y. Zhang, L. Yu, H. Sun and L. Zhang, *ACS Macro Lett.*, 2019, **8**, 205–212.
24 S. Boissé, J. Rieger, K. Belal, A. Di-Cicco, P. Beaunier, M.-H. Li and B. Charleux, *Chem. Commun.*, 2010, **46**, 1950–1952.
25 X. Zhang, S. P. Boissé, W. Zhang, P. Beaunier, F. D'Agosto, J. Rieger and B. Charleux, *Macromolecules*, 2011, **44**, 4149–4158.
26 W. Zhang, F. D'Agosto, O. Boyron, J. Rieger and B. Charleux, *Macromolecules*, 2012, **45**, 4075–4084.
27 J. Lesage de la Haye, X. Zhang, I. Chaduc, F. Brunel, M. Lansalot and F. D'Agosto, *Angew. Chem., Int. Ed.*, 2016, **55**, 3739–3743.

28 S. Y. Khor, N. P. Truong, J. F. Quinn, M. R. Whittaker and T. P. Davis, *ACS Macro Lett.*, 2017, **6**, 1013–1019.
29 J. C. Foster, S. Varlas, B. Couturaud, Z. Coe and R. K. O'Reilly, *J. Am. Chem. Soc.*, 2019, **141**, 2742–2753.
30 B. Charleux, G. Delaittre, J. Rieger and F. D'Agosto, *Macromolecules*, 2012, **45**, 6753–6765.
31 N. J. W. Penfold, J. Yeow, C. Boyer and S. P. Armes, *ACS Macro Lett.*, 2019, **8**, 1029–1054.
32 P. B. Zetterlund, S. C. Thickett, S. Perrier, E. Bourgeat-Lami and M. Lansalot, *Chem. Rev.*, 2015, **115**, 9745–9800.
33 J. Jennings, G. He, S. M. Howdle and P. B. Zetterlund, *Chem. Soc. Rev.*, 2016, **45**, 5055–5084.
34 D. Le, D. Keller and G. Delaittre, *Macromol. Rapid Commun.*, 2019, **40**, 1800551.
35 M. Lansalot, J. Rieger and F. D'Agosto, in *Macromolecular Self-Assembly*, ed. L. Billon and O. Borisov, John Wiley & Sons, Inc., New Jersey, 2016, p. 33.
36 W. M. Cai, W. M. Wan, C. Y. Hong, C. Q. Huang and C. Y. Pan, *Soft Matter*, 2010, **6**, 5554–5561.
37 J. T. Sun, C. Y. Hong and C. Y. Pan, *Polym. Chem.*, 2013, **4**, 873–881.
38 M. Huo, M. Zeng, D. Li, L. Liu, Y. Wei and J. Yuan, *Macromolecules*, 2017, **50**, 8212–8220.
39 Y. Zhang, G. Han, M. Cao, T. Guo and W. Zhang, *Macromolecules*, 2018, **51**, 4397–4406.
40 D. Li, M. Huo, L. Liu, M. Zeng, X. Chen, X. Wang and J. Yuan, *Macromol. Rapid Commun.*, 2019, **40**, 1900202.
41 Z. An, Q. Shi, W. Tang, C. K. Tsung, C. J. Hawker and G. D. Stucky, *J. Am. Chem. Soc.*, 2007, **129**, 14493–14499.
42 G. Zheng and C. Pan, *Macromolecules*, 2006, **39**, 95–102.
43 J. Rieger, F. O. Stoffelbach, C. Bu, D. Alaimo, C. Jérôme and B. Charleux, *Macromolecules*, 2008, **41**, 4065–4068.
44 W. M. Wan, X. L. Sun and C. Y. Pan, *Macromolecules*, 2009, **42**, 4950–4952.
45 G. Delaittre, C. Dire, J. Rieger, J. L. Putaux and B. Charleux, *Chem. Commun.*, 2009, 2887–2889.
46 Y. T. Li and S. P. Armes, *Angew. Chem., Int. Ed.*, 2010, **49**, 4042–4046.
47 W. J. Zhang, C. Y. Hong and C. Y. Pan, *Macromol. Rapid Commun.*, 2015, **36**, 1428–1436.
48 W. J. Zhang, C. Y. Hong and C. Y. Pan, *Biomacromolecules*, 2017, **18**, 1210–1217.
49 F. Lv, Z. An and P. Wu, *Nat. Commun.*, 2019, **10**, 1397.
50 M. J. Rymaruk, S. J. Hunter, C. T. O'Brien, S. L. Brown, C. N. Williams and S. P. Armes, *Macromolecules*, 2019, **52**, 2822–2832.
51 J. Wang, M. Cao, P. Zhou and G. Wang, *Macromolecules*, 2020, **53**, 3157–3165.
52 C. Gonzato, M. Semsarilar, E. R. Jones, F. Li, G. J. Krooshof, P. Wyman, O. O. Mykhaylyk, R. Tuinier and S. P. Armes, *J. Am. Chem. Soc.*, 2014, **136**, 11100–11106.
53 L. Yu, X. Dai, Y. Zhang, Z. Zeng, L. Zhang and J. Tan, *Macromolecules*, 2019, **52**, 7267–7277.
54 L. Yu, Y. Zhang, X. Dai, L. Zhang and J. Tan, *Chem. Commun.*, 2019, **55**, 7848–7851.
55 Y. Zhang, L. Yu, X. Dai, L. Zhang and J. Tan, *ACS Macro Lett.*, 2019, **8**, 1102–1109.
56 S. Sugihara, A. Blanazs, S. P. Armes, A. J. Ryan and A. L. Lewis, *J. Am. Chem. Soc.*, 2011, **133**, 15707–15713.
57 X. Wang and Z. An, *Macromol. Rapid Commun.*, 2019, **40**, 1800325.
58 Y. Yang, J. Zheng, S. Man, X. Sun and Z. An, *Polym. Chem.*, 2018, **9**, 824–827.
59 M. Chen, J. W. Li, W. J. Zhang, C. Y. Hong and C. Y. Pan, *Macromolecules*, 2019, **52**, 1140–1149.
60 X. F. Xu, C. Y. Pan, W. J. Zhang and C. Y. Hong, *Macromolecules*, 2019, **52**, 1965–1975.
61 F. Lv, Z. An and P. Wu, *Macromolecules*, 2019, **53**, 367–373.
62 S. Qu, R. Liu, W. Duan and W. Zhang, *Macromolecules*, 2019, **52**, 5168–5176.
63 M. Guerre, M. Semsarilar, F. Godiard, B. Améduri and V. Ladmiral, *Polym. Chem.*, 2017, **8**, 1477–1487.
64 G. Delaittre, J. Nicolas, C. Lefay, M. Save and B. Charleux, *Chem. Commun.*, 2005, 614–616.
65 G. Delaittre, J. Nicolas, C. Lefay, M. Save and B. Charleux, *Soft Matter*, 2006, **2**, 223–231.
66 G. Delaittre, M. Save and B. Charleux, *Macromol. Rapid Commun.*, 2007, **28**, 1528–1533.
67 S. G. N. Brusseau, F. D'Agosto, S. P. Magnet, L. Couvreur, C. C. Chamignon and B. Charleux, *Macromolecules*, 2011, **44**, 5590–5598.
68 E. Groison, S. Brusseau, F. D'Agosto, S. Magnet, R. Inoubli, L. Couvreur and B. Charleux, *ACS Macro Lett.*, 2011, **1**, 47–51.
69 G. Delaittre, M. Save, M. Gaborieau, P. Castignolles, J. Rieger and B. Charleux, *Polym. Chem.*, 2012, **3**, 1526–1538.
70 J. T. Sun, C. Y. Hong and C. Y. Pan, *Soft Matter*, 2012, **8**, 7753–7767.
71 X. G. Qiao, M. Lansalot, E. Bourgeat-Lami and B. Charleux, *Macromolecules*, 2013, **46**, 4285–4295.
72 E. Yoshida, *Colloid Polym. Sci.*, 2013, **291**, 2733–2739.
73 A. Darabi, A. R. Shirin-Abadi, J. Pinaud, P. G. Jessop and M. F. Cunningham, *Polym. Chem.*, 2014, **5**, 6163–6170.
74 X. G. Qiao, P. Y. Dugas, B. Charleux, M. Lansalot and E. Bourgeat-Lami, *Macromolecules*, 2015, **48**, 545–556.
75 D. Keller, A. Beloqui, M. Martinez-Martinez, M. Ferrer and G. Delaittre, *Biomacromolecules*, 2017, **18**, 2777–2788.
76 X. G. Qiao, O. Lambert, J. C. Taveau, P. Y. Dugas, B. Charleux, M. Lansalot and E. Bourgeat-Lami, *Macromolecules*, 2017, **50**, 3796–3806.
77 K. H. Kim, J. Kim and W. H. Jo, *Polymer*, 2005, **46**, 2836–2840.
78 W.-M. Wan and C.-Y. Pan, *Macromolecules*, 2007, **40**, 8897–8905.
79 S. Sugihara, S. P. Armes and A. L. Lewis, *Angew. Chem., Int. Ed.*, 2010, **49**, 3500–3503.
80 S. Sugihara, K. Sugihara, S. P. Armes, H. Ahmad and A. L. Lewis, *Macromolecules*, 2010, **43**, 6321–6329.
81 A. Blanazs, N. J. Warren, A. L. Lewis, S. P. Armes and A. J. Ryan, *Soft Matter*, 2011, **7**, 6399–6403.

82 V. Kapishon, R. A. Whitney, P. Champagne, M. F. Cunningham and R. J. Neufeld, *Biomacromolecules*, 2015, **16**, 2040–2048.
83 G. Wang, M. Schmitt, Z. Wang, B. Lee, X. Pan, L. Fu, J. Yan, S. Li, G. Xie, M. R. Bockstaller and K. Matyjaszewski, *Macromolecules*, 2016, **49**, 8605–8615.
84 M. Obeng, A. H. Milani, M. S. Musa, Z. Cui, L. A. Fielding, L. Farrand, M. Goulding and B. R. Saunders, *Soft Matter*, 2017, **13**, 2228–2238.
85 G. Wang, Z. Wang, B. Lee, R. Yuan, Z. Lu, J. Yan, X. Pan, Y. Song, M. R. Bockstaller and K. Matyjaszewski, *Polymer*, 2017, **129**, 57–67.
86 K. Wang, Y. Wang and W. Zhang, *Polym. Chem.*, 2017, **8**, 6407–6415.
87 M. Cao, Y. Zhang, J. Wang, X. Fan and G. Wang, *Macromol. Rapid Commun.*, 2019, **40**, 1900296.
88 S. Qu, K. Wang, H. Khan, W. Xiong and W. Zhang, *Polym. Chem.*, 2019, **10**, 1150–1157.
89 B. Shi, H. Zhang, Y. Liu, J. Wang, P. Zhou, M. Cao and G. Wang, *Macromol. Rapid Commun.*, 2019, **40**, 1900547.
90 J. Wang, Z. Wu, G. Wang and K. Matyjaszewski, *Macromol. Rapid Commun.*, 2019, **40**, 1800332.
91 Y. Wang, G. Han, W. Duan and W. Zhang, *Macromol. Rapid Commun.*, 2019, **40**, 1800140.
92 H. Tanaka, K. Yamauchi, H. Hasegawa, N. Miyamoto, S. Koizumi and T. Hashimoto, *Physica B*, 2006, **385–386**, 742–744.
93 K. Yamauchi, H. Hasegawa, T. Hashimoto, H. Tanaka, R. Motokawa and S. Koizumi, *Macromolecules*, 2006, **39**, 4531–4539.
94 X. Wang, J. E. Hall, S. Warren, J. Krom, J. M. Magistrelli, M. Rackaitis and G. G. A. Bohm, *Macromolecules*, 2007, **40**, 499–508.
95 Y. Zhao, N. Miyamoto, S. Koizumi and T. Hashimoto, *Macromolecules*, 2010, **43**, 2948–2959.
96 A. Alegria, R. Lund, F. Barroso-Bujans, A. Arbe and J. Colmenero, *Colloid Polym. Sci.*, 2014, **292**, 1863–1876.
97 D. J. Lunn, J. R. Finnegan and I. Manners, *Chem. Sci.*, 2015, **6**, 3663–3673.
98 C. E. Boott, J. Gwyther, R. L. Harniman, D. W. Hayward and I. Manners, *Nat. Chem.*, 2017, **9**, 785–792.
99 L. Zhang, C. Song, J. Yu, D. Yang and M. Xie, *J. Polym. Sci., Part A: Polym. Chem.*, 2010, **48**, 5231–5238.
100 J. Liu, Y. Liao, X. He, J. Yu, L. Ding and M. Xie, *Macromol. Chem. Phys.*, 2011, **212**, 55–63.
101 S. Varlas, J. C. Foster and R. K. O'Reilly, *Chem Commun*, 2019, **55**, 9066–9071.
102 K. Y. Yoon, I. H. Lee, K. O. Kim, J. Jang, E. Lee and T. L. Choi, *J. Am. Chem. Soc.*, 2012, **134**, 14291–14294.
103 K. Y. Yoon, I. H. Lee and T. L. Choi, *RSC Adv.*, 2014, **4**, 49180–49185.
104 W. Liu, X. Liao, Y. Li, Q. Zhao, M. Xie and R. Sun, *Chem. Commun.*, 2015, **51**, 15320–15323.
105 K. Y. Yoon, S. Shin, Y. J. Kim, I. Kim, E. Lee and T. L. Choi, *Macromol. Rapid Commun.*, 2015, **36**, 1069–1074.
106 J. Lim, Y. Cho, E. H. Kang, S. Yang, J. Pyun, T. L. Choi and K. Char, *Chem. Commun.*, 2016, **52**, 2485–2488.
107 E. H. Kang, S. Yang, S. Y. Yu, J. Kim and T. L. Choi, *J. Polym. Sci., Part A: Polym. Chem.*, 2017, **55**, 3058–3066.
108 D. B. Wright, M. A. Touve, L. Adamiak and N. C. Gianneschi, *ACS Macro Lett.*, 2017, **6**, 925–929.
109 J. Chen, R. Sun, X. Liao, H. Han, Y. Li and M. Xie, *Macromolecules*, 2018, **51**, 10202–10213.
110 J. Chen, Y. Wang, H. Li, H. Han, X. Liao, R. Sun, X. Huang and M. Xie, *Chem. Mater.*, 2018, **30**, 1102–1112.
111 J. C. Foster, S. Varlas, L. D. Blackman, L. A. Arkinstall and R. K. O'Reilly, *Angew. Chem., Int. Ed.*, 2018, **57**, 10672–10676.
112 D. B. Wright, M. A. Touve, M. P. Thompson and N. C. Gianneschi, *ACS Macro Lett.*, 2018, **7**, 401–405.
113 D. Le, M. Dilger, V. Pertici, S. Diabate, D. Gigmes, C. Weiss and G. Delaittre, *Angew. Chem.*, 2019, **58**, 4725–4731.
114 O. L. Torres-Rocha, X. Wu, C. Zhu, C. M. Crudden and M. F. Cunningham, *Macromol. Rapid Commun.*, 2019, **40**, 1800326.
115 S. Varlas, J. C. Foster, L. A. Arkinstall, J. R. Jones, R. Keogh, R. T. Mathers and R. K. O'Reilly, *ACS Macro Lett.*, 2019, **8**, 466–472.
116 D. B. Wright, M. T. Proetto, M. A. Touve and N. C. Gianneschi, *Polym. Chem.*, 2019, **10**, 2996–3000.
117 D. B. Wright, M. P. Thompson, M. A. Touve, A. S. Carlini and N. C. Gianneschi, *Macromol. Rapid Commun.*, 2019, **40**, 1800467.
118 W. M. Wan, C. Y. Hong and C. Y. Pan, *Chem. Commun.*, 2009, 5883–5885.
119 W. D. He, X. L. Sun, W. M. Wan and C. Y. Pan, *Macromolecules*, 2011, **44**, 3358–3365.
120 G. M. Whitesides and B. Grzybowski, *Science*, 2002, **295**, 2418–2421.
121 J. W. Liu, H. W. Liang and S. H. Yu, *Chem. Rev.*, 2012, **112**, 4770–4799.
122 M. J. Derry, L. A. Fielding and S. P. Armes, *Prog. Polym. Sci.*, 2016, **52**, 1–18.
123 J. Rieger, *Macromol. Rapid Commun.*, 2015, **36**, 1458–1471.
124 J. Zhou, H. Yao and J. Ma, *Polym. Chem.*, 2018, **9**, 2532–2561.
125 F. D'Agosto, J. Rieger and M. Lansalot, *Angew. Chem., Int. Ed.*, 2020, **59**, 2–27.
126 N. J. Warren and S. P. Armes, *J. Am. Chem. Soc.*, 2014, **136**, 10174–10185.
127 S. L. Canning, G. N. Smith and S. P. Armes, *Macromolecules*, 2016, **49**, 1985–2001.
128 A. B. Lowe, *Polymer*, 2016, **106**, 161–181.
129 W. J. Zhang, C. Y. Hong and C. Y. Pan, *Macromolecules*, 2014, **47**, 1664–1671.
130 P. B. Zetterlund, F. Aldabbagh and M. Okubo, *J. Polym. Sci., Part A: Polym. Chem.*, 2009, **47**, 3711–3728.
131 Q. Zhang and S. Zhu, *ACS Macro Lett.*, 2015, **4**, 755–758.
132 C. Gao, H. Zhou, Y. Qu, W. Wang, H. Khan and W. Zhang, *Macromolecules*, 2016, **49**, 3789–3798.
133 W. M. Wan, X. L. Sun and C. Y. Pan, *Macromol. Rapid Commun.*, 2010, **31**, 399–404.

134 C. Q. Huang and C. Y. Pan, *Polymer*, 2010, **51**, 5115–5121.
135 W. Cai, W. Wan, C. Hong, C. Huang and C. Pan, *Soft Matter*, 2010, **6**, 5554–5561.
136 J. Zhou, W. Zhang, C. Hong and C. Pan, *Polym. Chem.*, 2016, **7**, 3259–3267.
137 M. J. Derry, O. O. Mykhaylyk and S. P. Armes, *Angew. Chem., Int. Ed.*, 2017, **56**, 1746–1750.
138 A. Blanazs, J. Madsen, G. Battaglia, A. J. Ryan and S. P. Armes, *J. Am. Chem. Soc.*, 2011, **133**, 16581–16587.
139 R. Deng, M. J. Derry, C. J. Mable, Y. Ning and S. P. Armes, *J. Am. Chem. Soc.*, 2017, **139**, 7616–7623.
140 X. Chen, L. Liu, M. Huo, M. Zeng, L. Peng, A. Feng, X. Wang and J. Yuan, *Angew. Chem., Int. Ed.*, 2017, **56**, 16541–16545.
141 G. Mellot, J. M. Guigner, L. Bouteiller, F. Stoffelbach and J. Rieger, *Angew. Chem.*, 2019, **58**, 3173–3177.
142 J. Tan, X. Li, R. Zeng, D. Liu, Q. Xu, J. He, Y. Zhang, X. Dai, L. Yu, Z. Zeng and L. Zhang, *ACS Macro Lett.*, 2018, **7**, 255–262.
143 D. Liu, J. He, L. Zhang and J. Tan, *ACS Macro Lett.*, 2019, **8**, 1660–1669.
144 J. He, J. Cao, Y. Chen, L. Zhang and J. Tan, *ACS Macro Lett.*, 2020, **9**, 533–539.
145 J. Tan, X. Rao, J. Yang and Z. Zeng, *Macromolecules*, 2013, **46**, 8441–8448.
146 Y. Jiang, N. Xu, J. Han, Q. Yu, L. Guo, P. Gao, X. Lu and Y. Cai, *Polym. Chem.*, 2015, **6**, 4955–4965.
147 J. Tan, H. Sun, M. Yu, B. S. Sumerlin and L. Zhang, *ACS Macro Lett.*, 2015, **4**, 1249–1253.
148 P. Gao, H. Cao, Y. Ding, M. Cai, Z. Cui, X. Lu and Y. Cai, *ACS Macro Lett.*, 2016, **5**, 1327–1331.
149 J. Tan, D. Liu, Y. Bai, C. Huang, X. Li, J. He, Q. Xu and L. Zhang, *Macromolecules*, 2017, **50**, 5798–5806.
150 L. Huang, Y. Ding, Y. Ma, L. Wang, Q. Liu, X. Lu and Y. Cai, *Macromolecules*, 2019, **52**, 4703–4712.
151 Y. Ma, P. Gao, Y. Ding, L. Huang, L. Wang, X. Lu and Y. Cai, *Macromolecules*, 2019, **52**, 1033–1041.
152 Y. Z. You, C. Y. Hong and C. Y. Pan, *Chem. Commun.*, 2002, 2800–2801.
153 C. Ding, C. Fan, G. Jiang, X. Pan, Z. Zhang, J. Zhu and X. Zhu, *Macromol. Rapid Commun.*, 2015, **36**, 2181–2185.
154 T. G. McKenzie, Q. Fu, E. H. H. Wong, D. E. Dunstan and G. G. Qiao, *Macromolecules*, 2015, **48**, 3864–3872.
155 T. G. McKenzie, E. H. H. Wong, Q. Fu, A. Sulistio, D. E. Dunstan and G. G. Qiao, *ACS Macro Lett.*, 2015, **4**, 1012–1016.
156 S. Shanmugam, J. Xu and C. Boyer, *J. Am. Chem. Soc.*, 2015, **137**, 9174–9185.
157 C. Ding, J. Wang, W. Zhang, X. Pan, Z. Zhang, W. Zhang, J. Zhu and X. Zhu, *Polym. Chem.*, 2016, **7**, 7370–7374.
158 J. Wang, M. Rivero, A. Muñoz Bonilla, J. Sanchez-Marcos, W. Xue, G. Chen, W. Zhang and X. Zhu, *ACS Macro Lett.*, 2016, **5**, 1278–1282.
159 Q. Fu, K. Xie, T. G. McKenzie and G. G. Qiao, *Polym. Chem.*, 2017, **8**, 1519–1526.
160 J. Xu, K. Jung, A. Atme, S. Shanmugam and C. Boyer, *J. Am. Chem. Soc.*, 2014, **136**, 5508–5519.
161 J. Xu, K. Jung and C. Boyer, *Macromolecules*, 2014, **47**, 4217–4229.
162 J. Yeow, J. Xu and C. Boyer, *ACS Macro Lett.*, 2015, **4**, 984–990.
163 J. Zhou, C. Hong and C. Pan, *Mater. Chem. Front.*, 2017, **1**, 1200–1206.
164 J. Yeow, S. Shanmugam, N. Corrigan, R. P. Kuchel, J. Xu and C. Boyer, *Macromolecules*, 2016, **49**, 7277–7285.
165 N. Zaquen, W. A. A. W. Azizi, J. Yeow, R. P. Kuchel, T. Junkers, P. B. Zetterlund and C. Boyer, *Polym. Chem.*, 2019, **10**, 2406–2414.
166 N. Zaquen, J. Yeow, T. Junkers, C. Boyer and P. B. Zetterlund, *Macromolecules*, 2018, **51**, 5165–5172.
167 D. Liu, W. Cai, L. Zhang, C. Boyer and J. Tan, *Macromolecules*, 2020, **53**, 1212–1223.
168 B. Zhang, X. Wang, A. Zhu, K. Ma, Y. Lv, X. Wang and Z. An, *Macromolecules*, 2015, **48**, 7792–7802.
169 J. Tan, Q. Xu, X. Li, J. He, Y. Zhang, X. Dai, L. Yu, R. Zeng and L. Zhang, *Macromol. Rapid Commun.*, 2018, **39**, 1700871.
170 L. Yu, Y. Zhang, X. Dai, Q. Xu, L. Zhang and J. Tan, *Chem. Commun.*, 2019, **55**, 11920–11923.
171 J. R. M. Gromada and K. Matyjaszewski, *Macromolecules*, 2001, **34**, 7664–7671.
172 W. Jakubowski and K. Matyjaszewski, *Macromolecules*, 2005, **38**, 4139–4146.
173 K. Min, H. Gao and K. Matyjaszewski, *J. Am. Chem. Soc.*, 2005, **127**, 3825–3830.
174 D. Konkolewicz, A. J. D. Magenau, S. E. Averick, A. Simakova, H. He and K. Matyjaszewski, *Macromolecules*, 2012, **45**, 4461–4468.
175 A. Simakova, S. E. Averick, D. Konkolewicz and K. Matyjaszewski, *Macromolecules*, 2012, **45**, 6371–6379.
176 D. Konkolewicz, P. Krys, J. R. Góis, P. V. Mendonça, M. Zhong, Y. Wang, A. Gennaro, A. A. Isse, M. Fantin and K. Matyjaszewski, *Macromolecules*, 2014, **47**, 560–570.
177 J. Nicolas, B. Charleux, O. Guerret and S. Magnet, *Angew. Chem., Int. Ed.*, 2004, **43**, 6186–6189.
178 J. Jiang, X. Zhang, Z. Fan and J. Du, *ACS Macro Lett.*, 2019, **8**, 1216–1221.
179 C. Grazon, P. Salas-Ambrosio, E. Ibarboure, A. Buol, E. Garanger, M. W. Grinstaff, S. Lecommandoux and C. Bonduelle, *Angew. Chem.*, 2020, **59**, 622–626.
180 J. G. Murray and F. C. Schwab, *Ind. Eng. Chem. Prod. Res. Dev.*, 1982, **21**, 93–96.
181 O. Okay and W. Funke, *Macromolecules*, 1990, **23**, 2623–2628.
182 J. Kim, S. Y. Jeong, K. U. Kim, Y. H. Ahn and R. P. Quirk, *J. Polym. Sci., Part A: Polym. Chem.*, 1996, **34**, 3277–3288.
183 C. Zhou, J. Wang, P. Zhou and G. Wang, *Polym. Chem.*, 2020, **11**, 2635–2639.
184 M. Okubo, Y. Sugihara, Y. Kitayama, Y. Kagawa and H. Minami, *Macromolecules*, 2009, **42**, 1979–1984.
185 Y. Kitayama, A. Chaiyasat, H. Minami and M. Okubo, *Macromolecules*, 2010, **43**, 7465–7471.

186 Y. Kitayama, A. Chaiyasat and M. Okubo, *Macromol. Symp.*, 2010, **288**, 25–32.
187 Y. Kitayama, H. Moribe, H. Minami and M. Okubo, *Polymer*, 2011, **52**, 2729–2734.
188 H. Moribe, Y. Kitayama, T. Suzuki and M. Okubo, *Macromolecules*, 2011, **44**, 263–268.
189 Y. Kitayama, H. Moribe, K. Kishida and M. Okubo, *Polym. Chem.*, 2012, **3**, 1555–1559.
190 J. Sarkar, L. Xiao, A. W. Jackson, A. M. van Herk and A. Goto, *Polym. Chem.*, 2018, **9**, 4900–4907.
191 Q. Xu, C. Tian, L. Zhang, Z. Cheng and X. Zhu, *Macromol. Rapid Commun.*, 2019, **40**, 1800327.
192 H. Li, Q. Xu, X. Xu, L. Zhang, Z. Cheng and X. Zhu, *Polymers*, 2020, **12**, 150.
193 M. Zeng, X. Cao, H. Xu, W. Gan, B. D. Smith, H. Gao and J. Yuan, *Polym. Chem.*, 2020, **11**, 936–943.
194 R. Yin, D. Sahoo, F. Xu, W. Huang and Y. Zhou, *Polym. Chem.*, 2020, **11**, 2312–2317.
195 J. Chen, S. Cai, R. Wang, S. Wang, J. Zhang and X. Wan, *Macromolecules*, 2020, **53**, 1638–1644.